

Optimal control of a probabilistic dynamic for epidemic spreading in arbitrary complex networks

Fabrizio Angaroni^{1,2}

¹Center for Nonlinear and Complex Systems, Dipartimento di Scienza e Alta Tecnologia,
Università degli Studi dell’Insubria, via Valleggio 11, 22100 Como, Italy.

²Istituto Nazionale di Fisica Nucleare, Sezione di Milano, via Celoria 16, 20133 Milano, Italy.

PRE-PRINT-VERSION

This paper presents a discrete time probabilistic dynamic for simulating a contact-based epidemic spreading based on discrete time Markov chain process, in particular the attention is addressed to the susceptible-infectious-removed (SIR) model and the phase diagram of such model will be presented. Then, this report presents the set of equations that represent the optimal control strategies, by the means of Pontryagin’s maximum principle, in two different cases a vaccination policy and a combined vaccination-hospitalization policy and show a numerical simulation, with the standard forward-backward sweep procedure, for these equations.

I. INTRODUCTION

Modeling how diseases spread among individuals was introduced by Kermack and McKendrick [18, 19, 25] in 1927; they introduced a model known as the susceptible-infectious-removed (SIR) epidemic model, and they supposed that individuals of a population could be divided into three non-intersecting classes: susceptible who are healthy but can contract the disease, infectious individuals who have contracted the disease and can transmit it, and removed individuals who have recovered and cannot contract the disease anymore. If the epidemics is assumed to be Markoffian and proceeds via infection of nearest neighbors, then the relations that represent the SIR model are

$$\begin{aligned} S + I &\rightarrow I + I, \\ I &\rightarrow R. \end{aligned} \quad (1)$$

This kind of problem is called the general epidemic process (GEP) [10]; it is a stochastic multiparticle process that describes a vast number of phenomena in nature; for example, a simple stochastic and space-dependent model in regular lattice could describe the fairy rings, chemical solitary waves [12, 15], percolation [14], forest fires, and contact-based epidemic spreading.

The study complex networks has provided a better tool study the GEP in complicated topology that describe the biological system: for example, scale-free networks can represent sexual contacts, the Internet, and many other social, technological, and biological networks [2, 7, 28].

One of the most important goals of these studies [29] is to find an optimal feedback control strategy to minimize the epidemics, and optimality in this case means balancing some control costs against performance. For example, the optimal solution could provide the best vaccination or hospitalization strategy to minimize the cost of an epidemic [6].

Most of the studies on this problem use the mean-field (MF) approximation [7, 29], and these kinds of studies

have evaluated the macroscopic feature of the system-like critical behavior and phase transition [21, 37]; however, MF is not designed to provide information about individual nodes. To obtain information at the individual level (microscopic) of description, it is necessary to use Monte Carlo (MC) simulations. The main problem of MC models is the computational effort needed to evaluate the expectation values of microscopic quantities. Another point against Monte Carlo approach is that the optimal solution must be found through a random search algorithm, and the computational effort could be cumbersome due to the dimension of the space of possible configurations of a complex network. In this paper, the microscopic Markov-chain approach (MMCA) [9] for the SIR model is presented, and the vaccinated class to the model is then added for the optimal control system for this model in two different cases: the first case considers only a vaccination of susceptible policy, and the second case only considers two possible control strategies: the vaccination of the susceptible and the hospitalization of the infected. Some numerical examples are also presented.

II. THE MODEL

Consider the dynamics of a SIR epidemic process over a complex network composed by N nodes and the example of compartments diagram that represent the SIR model shown in Figure 1 (top). The topology of the contacts of the network is completely determined by its adjacency matrix [7] \mathbf{A} . Without loss of generality, \mathbf{A} is assumed to be symmetric and its elements $a_{i,j}$ are assumed to be only two possible values: 0 and 1. This hypothesis is not necessary, and in general cases where the strength of the link is considered can be treated in the same manner of this work. Following the construction of Johnson [17] for a stochastic dynamic, a vector space \mathbb{V}_k $k = 1, \dots, N$ is associated with every node; and defining a basis, a non-

natural isomorphism $\mathbb{V}_k \simeq \mathbb{R}^{d_k}$ is built, and where d_k are the possible configurations of k -th node, which $d_k = d$ is supposed $\forall k$. Then, a vector that represents its state is attached to each node. For example, in the SIR model, the following state is obtained for every node:

$$\bar{v}_k(t_i) = \begin{bmatrix} S_k(t_i) \\ I_k(t_i) \\ R_k(t_i) \end{bmatrix}. \quad (2)$$

Components of vectors $A_k(t_i)$ for $A = S, I, R$ are treated as the probability that k -th node is in the configuration A at time t_i . This hypothesis implies that every $\bar{v}_k(t_i)$ is normalized by the means of the 1-norm, or

$$S_k(t_i) + I_k(t_i) + R_k(t_i) = 1. \quad (3)$$

In addition, the systems is represented by a state $\Lambda(t_i) \in \otimes_{k=1}^N \mathbb{V}_k$.

α is defined as the probability for the unit of time that an infectious individual spreads the disease to one of its neighbors and δ as the probability for unit of time that an infected node is removed. Then, the probability of node k not being infected by any neighbor is the following:

$$P_{0,k}(t_i) := \prod_{j=1}^N (1 - a_{k,j} \alpha I_j(t_k)), \quad (4)$$

and the discrete-time equation that describes the dynamics are given by

$$\begin{aligned} S_k(t_{i+1}) &= S_k(t_i) - (1 - P_{0,k}(t_i)) S_k(t_i), \\ I_k(t_{i+1}) &= I_k(t_i) + (1 - P_{0,k}(t_i)) S_k(t_i) - \delta I_k(t_i) \end{aligned} \quad (5)$$

$$R_k(t_{i+1}) = 1 - S_k(t_{i+1}) - I_k(t_{i+1})$$

This kind of formalism in [9] is called MMCA, since it is equivalent to associate a discrete time Markov chain for every node of the network; for example, see Figure 1 (bottom) for the microscopic Markov chain of the SIR model. The solution is easily obtained if initial conditions are given, and in [9], it is proven that this formalism can outperform heterogeneous MF (HMF) and MC approaches.

Equations 5 can always be solved if an initial condition is given, and it is possible to accommodate initial conditions with some grade of uncertainty, which is common dealing with real data.

It is known that the SIR model has two different phases [10, 11, 14, 21] (equilibrium states) for $t_{fin} \rightarrow \infty$, one where all the susceptible become infected or removed another where some susceptible manage to survive without contracting the disease.

III. SINGLE CONTROL

This section shows the construction of an optimal control system for the discrete time process presented in

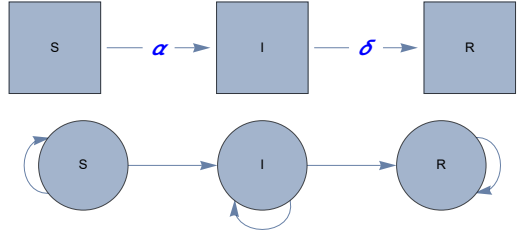


FIG. 1: SIR.

[5, 22, 32]. In addition, there is a policy maker that is supposed to be able to determine when it is necessary to vaccinate a node. To simulate this procedure, the vaccinated class was added to the system, and the model in this case is called susceptible-infectious-removed-vaccinated (SIRV) [25]; Now, the possible micro states of a node are $d = 4$. The set of admissible controls (possible actions of the policy makers) is assumed to be provided by the following:

$$\mathbb{U} = \{\omega_1(t_1), \dots, \omega_N(t_{fin}) | \forall j = 1, \dots, N, \forall l = 0, \dots, t_{fin}, 0 \leq \omega_j(t_l) \leq 1\}; \quad (6)$$

where $\omega_k(t_i)$ is the probability at time i that the k -th susceptible node becomes vaccinated; here some grade of failure of the therapy is assumed in fact it is possible that a vaccinated becomes infectious with probability $\gamma < \alpha$, this represents a non-efficacious vaccination [25] or a development of the resistance to the disease [33]. The probability of the vaccinated node k not being infected by any neighbor is defined as the following:

$$P_{0,k,V}(t_i) := \prod_{j=1}^N (1 - a_{k,j} \gamma I_j(t_k)), \quad (7)$$

where $V_k(t_i)$ is the probability that the k -th node is vaccinated at time t_i .

Then, the dynamics of the probabilities is driven by the following $4N$ finite difference time equations:

$$\begin{aligned} S_k(t_{i+1}) &= S_k(t_i) - (1 - P_{0,k}(t_i)) S_k(t_i) (1 - \omega_k(t_i)) \\ &\quad - P_{0,k}(t_i) \omega_k(t_i) S_k(t_i), \\ I_k(t_{i+1}) &= I_k(t_i) + (1 - P_{0,k}(t_i)) S_k(t_i) (1 - \omega_k(t_i)) \\ &\quad + (1 - P_{0,k,V}(t_i)) V_k(t_i) - \delta I_k(t_i) \\ V_k(t_{i+1}) &= V_k(t_i) - (1 - P_{0,k,V}(t_i)) V_k(t_i) \\ &\quad + P_{0,k}(t_i) S_k(t_i) \omega_k(t_i), \\ R_k(t_{i+1}) &= 1 - S_k(t_{i+1}) - I_k(t_{i+1}) - V_k(t_{i+1}). \end{aligned} \quad (8)$$

The last equation is obtained from the normalization condition. The compartment diagram for this model shown

in Figure 2 (left) instead of in Figure 2 (right) shows the microscopic Markov chain associated to every node of the complex network.

To proceed further, the following $3N$ functions must be defined:

$$\begin{aligned} g_{k,S}(t_i) &= S_k(t_{i+1}) - S_k(t_i) = \\ &= -S_k(t_i)(1 - P_{0,k})(1 - \omega_k(t_i))S_k(t_i) \\ &\quad - P_{0,k}\omega_k(t_i)S_k(t_i), \\ g_{k,I}(t_i) &= I_k(t_{i+1}) - I_k(t_i) = \\ &= (1 - P_{0,k}(t_i))(1 - \omega_k(t_i))S_k(t_i) \\ &\quad - \delta I_k(t_i) + (1 - P_{0,k,V}(t_i))V_k(t_i), \\ g_{k,V}(t_i) &= V_k(t_{i+1}) - V_k(t_i) = \\ &= -(1 - P_{k,0,V}(t_i))V_k(t_i) + P_{0,k}\omega_k(t_i)S_k(t_i). \end{aligned} \quad (9)$$

In addition, the cost must be defined:

$$J(\Lambda_{fin}, t_{fin}) := \sum_{k=1}^N \left[\phi_k(t_{fin}) + \sum_{j=0}^{t_{fin}-1} f_{j,k}(\Lambda_j, t_j) \right], \quad (10)$$

the first term represents a payoff given by the final state, while the second term represents a cumulative cost. Without loss of generality, the maximum is given by the following:

$$J(\Lambda_{fin}, t_{fin}) = - \sum_{k=1}^N \left[\sum_{j=0}^{t_{fin}-1} C_1 I_k(t_j) + \frac{C_2}{2} \omega_k^2(t_j) \right]. \quad (11)$$

This cost simulates when there is a cost associated to the vaccination and a cost associated to the infectious individuals, which, for example, can represent the loss of work days.

This definition fixes the behavior of the control, and it could be defined in a different manner to change the behavior of the policy maker, for example, see [6]. However, the only request is that the cost is quadratic in the control (i.e. $\omega_k(t_i)$), and the same procedure of this work could be used to consider more realistic costs. By choosing a finite horizon optimal control, adding a time discount to the cost creates an infinite horizon control. However, the first term of (11) gives a cost that increases with time due to the intrinsic dynamics of the system, so it is not necessary to use a time discount function. In addition, if cost depends onto $R_k(t_i)$, then it is not possible to determine $R_k(t_i)$ from the normalization condition.

Then, to build an optimal control system, a Hamiltonian must be defined:

$$H(t_i, \Lambda_i, \omega_i) = H_i = \sum_{k=1}^N [f_{k,i} + \lambda_{k,S}(t_{i+1})g_{k,S}(t_i)] \quad (12)$$

$$+ \lambda_{k,I}(t_{i+1})g_{k,I}(t_i) + \lambda_{k,V}(t_{i+1})g_{k,V}(t_i)], \quad (13)$$

where $\lambda_{k,A}(t_i)$ $A = S, I, V$ are the adjoint functions. First, the transversality conditions are given by the following:

$$\lambda_{k,A}(t_{fin}) = \frac{\partial \phi_k(t_{fin})}{\partial A_k(t_{fin})} = 0. \quad (14)$$

Then, from the definition (12), the adjoint functions for $t \neq t_{fin}$ are given by the following

$$\lambda_{k,S}(t_i) = \frac{\partial H_i}{\partial S_k(t_i)}, \quad (15)$$

$$\lambda_{k,I}(t_i) = \frac{\partial H_i}{\partial I_k(t_i)}, \quad (16)$$

$$\lambda_{k,V}(t_i) = \frac{\partial H_i}{\partial V_k(t_i)}. \quad (17)$$

Thus, the following recurrence relations are obtained for the adjoint functions by solving the previous equations:

$$\begin{aligned} \lambda_{k,S}(t_i) &= \lambda_{k,S}(t_{i+1})[-(1 - P_{0,k}(t_i))(1 - \omega_k(t_i)) \\ &\quad - P_{0,k}(t_i)\omega_k(t_i)] + \\ \lambda_{k,I}(t_{i+1}) &= [(1 - P_{0,k}(t_i))(1 - \omega_k(t_i)) \\ &\quad + \lambda_{k,V}(t_{i+1}P_{0,k}(t_i)\omega_k(t_i))], \end{aligned}$$

$$\begin{aligned} \lambda_{k,I}(t_i) &= C_1 - \delta \lambda_{k,I}(t_{i+1}) + \\ &\quad \sum_{j=1}^N \sum_{j \neq k} \{ + \lambda_{j,S}(t_{i+1}) \\ &\quad [(1 - \omega_j(t_i))S_k(t_i)h_{k,j}(t_i) \\ &\quad - \omega_j(t_i)S_j(t_i)h_{k,j}(t_i)] \\ &\quad - \lambda_{j,I}(t_{i+1})[(1 - \omega_j(t_i))S_j(t_i)h_{k,j}(t_i)) \\ &\quad + V_j(t_i)h_{k,j}(t_i)] + \\ &\quad + \lambda_{j,V}(t_{i+1})[V_j(t_i)h_{k,j}(t_i) \\ &\quad + S_j(t_i)\omega_j(t_i)h_{k,j}(t_i)] \}, \end{aligned} \quad (18)$$

$$\begin{aligned} \lambda_{k,V}(t_i) &= \lambda_{k,I}(t_{i+1})(1 - P_{0,k,V}(t_i)) \\ &\quad + \lambda_{k,V}(t_{i+1})(P_{0,k,V}(t_i) - 1) \end{aligned}$$

where $h_{k,j}(t_i)$ and $h_{k,j}(t_i)$ are given by the following:

$$h_{k,j}(t_i) = -a_{j,k}\alpha \prod_{l=1, l \neq k}^N (1 - a_{j,l}\alpha I_l(t_i)), \quad (19)$$

$$h_{k,j}(t_i) = -a_{j,k}\gamma \prod_{l=1, l \neq k}^N (1 - a_{j,l}\gamma I_l(t_i)). \quad (20)$$

Eventually, by applying the extension of Pontryagins maximum principle for discrete systems [30], the characterization of the optimal control is obtained, imposing $\frac{\partial H_i}{\partial \omega_k(t_i)} = 0$:

$$\omega_k^*(t_i) = \min\{\max\{0, K\}, 1\}, \quad (21)$$

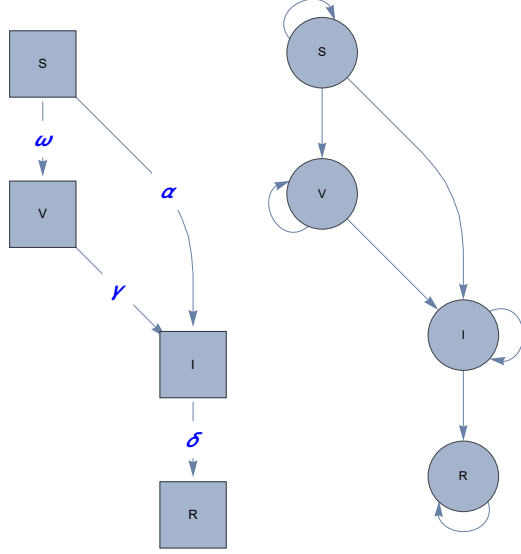


FIG. 2: At left there is the flowchart associated to the SIVR with one control, at right there is the MMC for this problem

with

$$K = \frac{1}{C_2} \{ \lambda_{k,S}(t_i + 1) [(1 - P_{0,k}(t_i)) S_k(t_i) - P_{0,k}(t_i) S_k(t_i)] + \lambda_{k,I}(t_i) [-(1 - P_{0,k}(t_i)) S_k(t_i)] + \lambda_{k,V}(t_i) P_{0,k} S_k(t_i) \}. \quad (22)$$

The optimality system in the state Equations (8) with initial conditions and adjoint Equations (18) with the final time conditions (transversality conditions) and with the characterization of the optimal control (22). Some numerical examples are also shown in section V

IV. DOUBLE CONTROL

Now, a more general case of a contact epidemic it is consider supposing that there is a natural time decay of the protection given by the vaccination, there is a probability (θ) for a unit of time that a vaccinated becomes susceptible. In addition, there are the possibility that the policy maker could cure an infected, for example, the hospitalization of a person with an infectious disease, this action is represented by a transition from infected to vaccinated. Thus, the probability for a unit of time of this event is given by the new set of control $\tau_k(t_i)$, there are $2N$ controls, and the set of possible actions of the policy maker is given by the following equation:

$$\mathbb{U} = \{\omega_1(t_1), \dots, \omega_N(t_{fin}), \tau_1(t_1), \dots, \tau_N(t_{fin})\} \quad (23)$$

$$\forall j = 1, \dots, N, \forall l = 0, \dots, t_{fin}, 0 \leq \omega_j(t_l) \leq 1, 0 \leq \tau_j(t_l) \leq 1\}$$

The compartment diagram for such system is presented in Figure 3 (top). Given the initial conditions, the discrete time dynamics of this system is completely specified

by the following $4N$ equations :

$$\begin{aligned} S_k(t_{i+1}) &= S_k(t_i) - (1 - P_{0,k}(t_i)) \\ &\quad (1 - \omega_k(t_i)) S_k(t_i) - P_{0,k} \omega_k(t_i) S_k(t_i) + \\ &\quad \theta V_k(t_i) P_{0,V,k}(t_i), \\ I_k(t_{i+1}) &= I_k(t_i) + (1 - P_{0,k}(t_i))(1 - \omega_k(t_i)) S_k(t_i) \\ &\quad + (1 - P_{0,V,k}(t_i))(1 - \theta) V_k(t_i) - (1 - \delta) \tau_k(t_i) I_k(t_i) \\ &\quad - \delta I_k(t_i)(1 - \tau_k(t_i)), \\ V_k(t_{i+1}) &= V_k(t_i) + P_{0,k}(t_i) \omega_k(t_i) S_k(t_i) \\ &\quad + (1 - \delta) \tau_k(t_i) I_k(t_i) \\ &\quad - (1 - P_{0,V,k}(t_i))(1 - \theta) V_k(t_i), \\ R_k(t_i) &= 1 - S_k(t_i) - I_k(t_i) - R_k(t_i). \end{aligned} \quad (24)$$

Again, these equations completely specify the time dynamics of the probability if initial (probabilistic) conditions are given. In Figure 3 (bottom), the microscopic Markov chain associated to Equations (24) is presented. In this case, the cost that is maximized in the following sections is the following:

$$J(\Lambda_{fin}, t_{fin}) = - \sum_{k=1}^N \left[\sum_{j=0}^{t_{fin}-1} C_1 I_k(t_j) + \frac{C_2}{2} \omega_k^2(t_j) + \frac{C_3}{2} \tau_k^2(t_j) \right]. \quad (25)$$

In this case, a term that can mimic hospitalization and drug treatment costs is used.

As performed in the previous section, a Hamiltonian can be defined to obtain the recurrence relations for the adjoint functions:

$$\begin{aligned} \lambda_{k,S}(t_i) &= \lambda_{k,S}(t_{i+1}) \\ &\quad [-(1 - P_{0,k}(t_i))(1 - \omega_k(t_i)) - P_{0,k}(t_i) \omega_k(t_i)] \\ &\quad + \lambda_{k,I}(t_{i+1})(1 - P_{0,k}(t_i))(1 - \omega_k(t_i)) + \lambda_{k,V}(t_{i+1}) P_{0,k}(t_i), \end{aligned}$$

$$\begin{aligned} \lambda_{k,I}(t_i) &= C_2 + \lambda_{k,V}(t_{i+1})(1 - \delta) \tau_k(t_i) \\ &\quad - \lambda_{k,I}(t_{i+1})(1 - \delta) \tau_k(t_i) \\ &\quad + \sum_{j=1, j \neq k}^N \{ \lambda_{j,S}(t_{i+1}) [S_j(t_i)(1 - \omega_j(t_i)) h_{j,k}(t_i) \\ &\quad - \omega_j(t_i) S_j(t_i) h_{j,k}(t_i) + \theta V_j(t_i) h v_{j,k}(t_i)] \\ &\quad + \lambda_{j,I}(t_{i+1}) [-(1 - \omega_j(t_i)) S_j(t_i) h_{j,k}(t_i) \\ &\quad - (1 - \theta) V_j(t_i) h v_{j,k}(t_i)] \\ &\quad + \lambda_{j,V}(t_{i+1}) [(1 - \theta) V_j(t_i) h_{j,k}(t_i) + \omega_k(t_i) S_k(t_i) h_{j,k}(t_i) \\ &\quad - \theta V_j(t_i) h v_{j,k}(t_i)] \}, \end{aligned} \quad (26)$$

$$\begin{aligned} \lambda_{k,V}(t_i) &= \lambda_{k,S}(t_{i+1}) \theta P_{0,V,k}(t_i) \\ &\quad + \lambda_{k,I}(t_{i+1})(1 - P_{0,V,k}(t_i))(1 - \theta) \\ &\quad + \lambda_{k,V}(t_{i+1}) [-(1 - P_{0,V,k}(t_i))(1 - \theta) - \theta P_{0,V,k}(t_i)], \end{aligned} \quad (27)$$

where the functions $h_{j,k}(t_i)$ and $h v_{j,k}(t_i)$ are defined in Equations (19) and (20). The transversality conditions are the same as previously given (see Equations (14)) Again, by imposing the following condition,

$$\frac{\partial H_i}{\partial \omega_k^*(t_i)} = 0, \quad \frac{\partial H_i}{\partial \tau_k^*(t_i)} = 0 \quad (28)$$

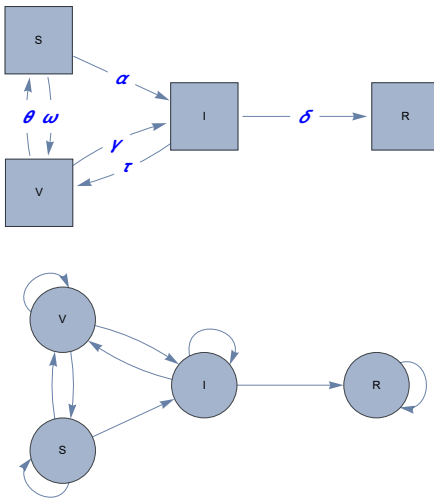


FIG. 3: At left there is the compartment diagram associated to the SIVR with double control, at bottom there is the MMC for this problem.

, the following $2N$ equations that characterize the optimal control are obtained:

$$\omega_k^*(t_i) = \min\{\max\{0, K\}, 1\}, \quad (29)$$

with

$$K = \frac{1}{C_2} \{ \lambda_{k,S}(t_i + 1) [(1 - P_{0,k}(t_i))S_k(t_i) - P_{0,k}(t_i)S_k(t_i)] + \lambda_{k,I}(t_i) [-(1 - P_{0,k}(t_i))S_k(t_i)] + \lambda_{k,V}(t_i)P_{0,k}S_k(t_i) \}, \quad (30)$$

$$\tau_k^*(t_i) = \min\{\max\{0, M\}, 1\}, \quad (31)$$

with

$$M = \frac{1}{C_3} \{ \lambda_{k,I}(t_i + 1) [-(1 - \delta)I_k(t_i) + \delta I_k(t_i)] + \lambda_{k,V}(t_i) [(1 - \delta)I_k(t_i)] \}. \quad (32)$$

The optimality system consists of state Equations (24) with initial conditions and adjoint Equations (26) with the final time conditions (transversality conditions) and with the characterizations of the optimal control (30) and (32).

V. NUMERICAL EXAMPLES

To show some examples, a random complex network with 30 nodes is first chosen such that the adjacency matrix is symmetric, $a_{i,j} = a_{j,i}$, $\forall i, j = 1, \dots, 30$. In addition, every node must have at least one connection with another node, and the reference complex network is shown in Figure 4.

Then, the initial condition is fixed by choosing random a

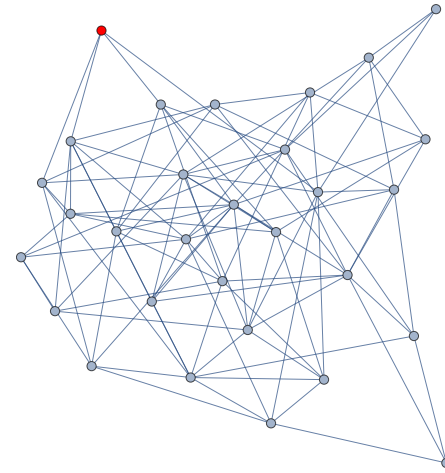


FIG. 4: Reference complex network used for numerical simulation. In red the node who starts infectious.

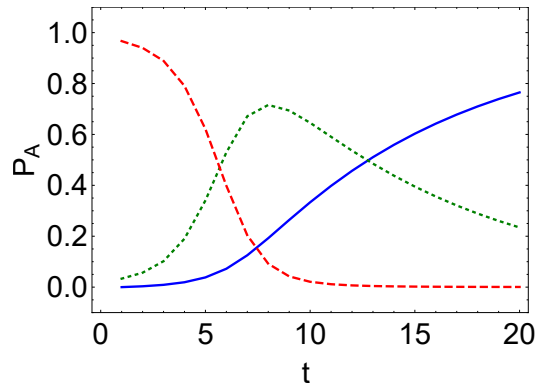


FIG. 5: Time dynamics of the probabilities in Equation (33) for the SIR dynamics with $\alpha = 0.2$ $\delta = 0.1$. The Red dashed line represents $P_S(t_i)$, the green dotted line represents $P_I(t_i)$, and the blue solid line represents $P_R(t_i)$. It is possible to notice that with these values of α and δ , susceptible-free equilibrium is reached for a sufficient time.

node and setting it as $I_k(t_0) = 1$. The last choice made corresponds to the constants, and they were set for the SIR model $\alpha = 0.2$ and $\delta = 0.1$. The choice of these constants and the network was made to assure that the system has critical behavior, in other words, for $t_{fin} \rightarrow \infty$, $R_k(t_{fin}) = 1 \quad \forall k = 1, \dots, 30$, which is the so called the susceptible-free equilibrium, in Figure 6, it is shown the phase diagram of SIR model in the reference network. In addition this behavior could be also seen in Figure 5, and these plots present the probability of a node to be susceptible, infected, or removed, and this quantity is defined as follows:

$$P_A(t_i) := \frac{1}{N} \sum_{k=1}^N A_k(t_i), \quad (33)$$

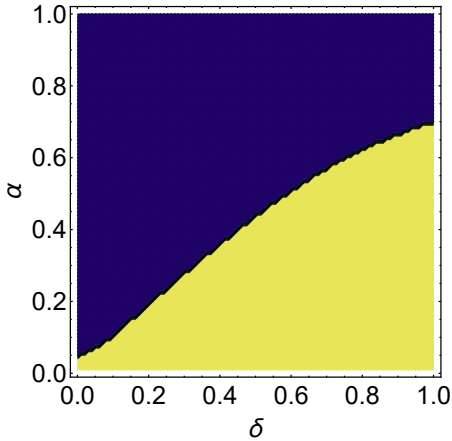


FIG. 6: Phase diagram of the SIR model in the reference network, in yellow the points in the parameters space of α and δ where there is a non negligible (greater than 10^{-5}) probability of the survival of a healthy susceptible, in blue the points of susceptible-free equilibrium.

with $A = R, I, S$ or V .

To obtain the optimal control, the standard forward-backward sweep method is applied, and the procedure is the following:

- Step 1. Create a guess for all controls.
- Step 2. Solve forward the dynamics of the system with the given control and initial conditions.
- Step 3. Solve backward in time the adjoint equations.
- Step 4. Evaluate new optimal conditions for controls.
- Step 5. Update the control with a weighted average between the old control and the controls evaluated in Step 4.
- Step 6. Check the convergence, if reached, stop; otherwise, go back to Step 2.

If l is the index that represents the iteration number of the procedure stated, the criterion of convergence for the case with one control is the following equation:

$$\forall k = 1, \dots, N \quad \forall k_i = 1 \dots, t_{fin}$$

$$\max\{\max\{\max\{|\omega_{k,l}(t_i) - \omega_{k,l+1}(t_i)|, |I_{k,l}(t_i) - I_{k,l+1}(t_i)|\}, |S_{k,l}(t_i) - S_{k,l+1}(t_i)|\}, |V_{k,l}(t_i) - V_{k,l+1}(t_i)|\} < \rho, \quad (34)$$

in contrast, for the case with double control, the stop criterion is given by the following equation:

$$\forall k = 1, \dots, N \quad \forall k_i = 1 \dots, t_{fin}$$

$$\max\{\max\{\max\{\max\{|\omega_{k,l}(t_i) - \omega_{k,l+1}(t_i)|, |I_{k,l}(t_i) - I_{k,l+1}(t_i)|\}, |S_{k,l}(t_i) - S_{k,l+1}(t_i)|\}, |V_{k,l}(t_i) - V_{k,l+1}(t_i)|\}, |\tau_{k,l}(t_i) - \tau_{k,l+1}(t_i)|\} < \rho, \quad (35)$$

in both cases, $\rho = 10^{-4}$. This criterion means that the process is stopped only when the maximum distance between states and controls of between two consecutive iterations is less than ρ .

Figure 7 shows the optimal solution of the SIRV problem with one control for different choices of the values of the constants in Equation (11). In contrast, Figure 8 shows the optimal solution of the SIRV problem with two controls for different choices of the values of the constants in Equation (11). The optimal solution could indicate a probabilistic vaccination of a node, since $0 \leq \omega_k(t_i) \leq 1$. This fact is not a problem if a node represents a metapopulation, but if a node represents a single individual, a partial vaccination is not understandable (and maybe ethically problematic). Attempts to solve this problem include using a binary control, but in this case, the hypothesis of a piecewise continuous cost fails, and the optimal solution could not be obtained.

Eventually to quantify the effects of the controls on the system the incidence is presented, we compare the time evolution of incidence in the three models taken in account, results are show in Figure 9, in this figure it is possible to notice the effects of optimal control in reducing the but that in the case of double control the optimal solution for $C_1 = C_2 = C_3$ is to leave a very small probability that a nodes is infected so the infectious disease become endemic in that complex network, the average probability of a node to be infected by an another node after 100 time steps is very low $\sim 7 \cdot 10^{-3}$ and this could not be true if the constants in the cost are estimated in an another way, however this behavior is due to the fact that in the double control model taken in account a vaccinated individual could become susceptible again, this feature gives “supplies” to the infected population as in the susceptible-infected-susceptible (SIS) model. Another fundamental contribution to this behavior is due to the fact the cost is quadratic in controls, and the controls are bounded between 0 and 1 so, distribuiting the action in more steps is “cheaper” than doing the same action in a lesser number of steps.

Another quantity common in epidemiology is the force of infection, defined in this case as $F(t_i) = \sum_{k=1}^N \alpha I_k(t_i)$, again it is clear the effects of controls in reducing the “size” of the infection, and again the double control model show an endemicity of the disease.

VI. CONCLUSION

Summarizing, the time discrete-time equations for the dynamics of the probability of individual nodes in the SIR model have been derived. In addition, this method outperforms HMF and MC simulation [9], since the proposed method requires small computational effort and can accommodate probabilistic (with some degree of uncertain) initial conditions that are common in epidemiology studies [4, 26].

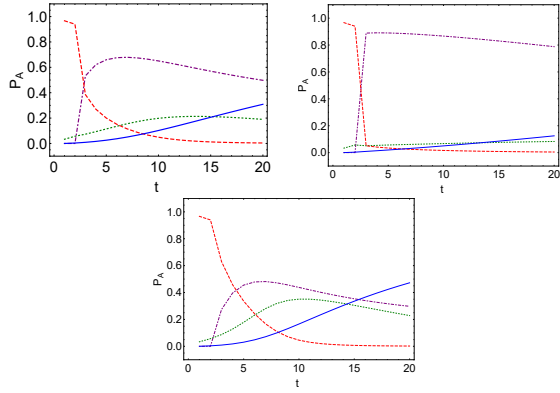


FIG. 7: Time dynamics of the probabilities in Equation (33) for the SIRV dynamics with only vaccination control $\omega_k(t_I)$, the values used for the constant are $\alpha = 0.2$, $\delta = 0.1$, and $\gamma = 0.02$. Different values for the constants were tested in (11): top left $C_1 = C_2 = 1$, top right $C_1 = 2C_2 = 2$, and bottom $2C_1 = C_2 = 2$. The Red dashed line is $P_S(t_i)$, the green dotted line represents $P_I(t_i)$, the purple dot dashed line represents $P_V(t_i)$, and the blue solid line represents $P_R(t_i)$.

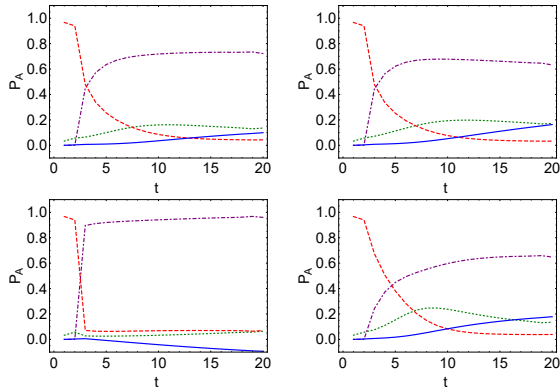


FIG. 8: Time dynamics of the probabilities in Equation (33) for the SIRV dynamics with both controls $\omega_k(t_I)$ and $\tau_k(t_I)$; the values used for the constant are $\alpha = 0.2$, $\delta = 0.1$, $\theta = 0.01$, and $\gamma = 0.02$. Different values for the constants were tested in (25): top left $C_1 = C_2 = C_3 = 1$, top right $C_3 = 2C_1 = 2C_2 = 2$, bottom right $2C_1 = C_2 = 2C_3 = 2$, and bottom left $C_1 = 2C_2 = 2C_3 = 2$. The Red dashed line represents $P_S(t_i)$, the green dotted line represents $P_I(t_i)$, the purple dot dashed line represents $P_V(t_i)$, and the blue solid line represents $P_R(t_i)$.

In addition, the framework for the SIRV was generalized, and the optimal control in two different cases was then studied, considering only a vaccination strategy (transition from susceptible to vaccinated) and a double control (transition from susceptible to vaccinated and a transition from infectious to vaccinated), this study presents the set of equations needed to obtain the

optimal control strategy given a cost, a network, and an

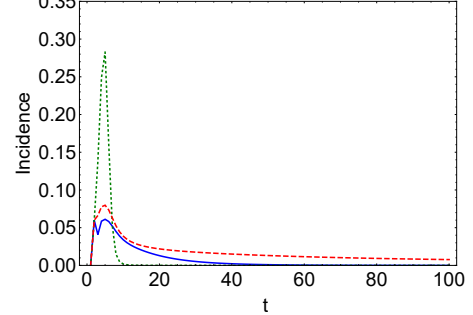


FIG. 9: The incidence in three different cases, Green dotted line is the incidence of SIR model , Blue straight line is the case of single control, and Red dashed line represents the case with two controls. In this case the following constant are chosen $\alpha = 0.2$, $\delta = 0.1$, $\gamma = 0.02$, $\theta = 0.01$ and $C_1 = C_2 = C_3 = 1$.

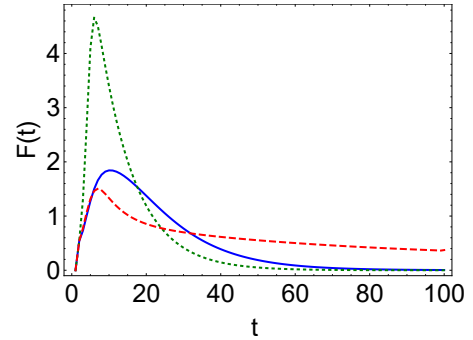


FIG. 10: The force of infection, $F(t_i) = \sum_{k=1}^N \alpha I_k(t_i)$, of the three different cases taken in account, Gen dotted line F_{t_i} of SIR model , Blue straight line is the case of single control, and Red dashed line represents the case with two controls. In this case the following constant are chosen $\alpha = 0.2$, $\delta = 0.1$, $\gamma = 0.02$, $\theta = 0.01$ and $C_1 = C_2 = C_3 = 1$.

initial probability distribution of infectious, susceptible, removed, and vaccinated.

This kind of simulation could give an insight of how to balance cost (e.g drugs production), epidemics constants (failure probability and duration of the vaccination), and distribution of health care in order to eradicate (or minimize) a endemic disease.

Further works are required to overcome the problem of a probabilistic treatment. This method will also be applied to studying an infectious plant disease. Since in this case the topology of the complex network is known and fixed in time, there is an interesting development of remote supervision [3, 8, 26] of the disease, and the only concern in this case is that the SIRV dynamics could be not appropriate [20] for simulating a plant disease, so a tailored dynamic could be required.

[1] O. N. Bjornstad, B. F. Finkenstad and B. T. Grenfeld, *Ecological Monographs*, 2002, **72**, pp 169-184.

[2] S. Boccaletti, V. Latora, Y. Moreno, M. Chavez and D.-U. Hwang, *Phys. Rep.* **424**, 175 (2006).

[3] P. Boursier, *International Journal of Engineering and Technology*, 2015, **11**.

[4] E. Christaki, *Virulence*, 2015, **6**, pp 558-565.

[5] W. Ding and R. Hendon and B. Cathey and E. Lancaster and R. Germick, *INVOLVE*, 2014, **7**.

[6] B. Dybiec, A. Kleczkowski and C.A. Gilligan, *ACTA PHYSICA POLONICA B*, 2005, **36**.

[7] M. Draief and L. Massoulié, *Epidemics and rumours in complex network*, 2010, Cambridge university press The Edinburgh Building, Cambridge CB2 8RU, UK.

[8] A. Fuentes, S. Yoon, S. C. Kim and D.S. Park, *Sensors*, 2017, **17**, 2022.

[9] S. Gomez, A. Arenas, J Borge-Holthoefer, S. Meloni and Y. Moreno, *Int. J. Complex Systems in Science*, 2011, **1**, pp 47 -54.

[10] P. Grassberger, *Mathematical Biosciences*, 1983, **63**, pp 157-172.

[11] P. Grassberger, *J. Phys. A: Math. Gen*, 1985, **18**, pp 267-271.

[12] A. Hanna and K. Showalter, talk at conference on non-linear phenomena in chemical dynamics, Bordeaux, Sept. 1981.

[13] Y. Hasan, U. J. Potter and R., *Cooper, Plant Pathology*, 2009, **58** , pp 982-989.

[14] S. Havlin, J. E. Kiefer, F. Leyvraz and G. H. Weiss, *Journal of Statistical Physics*, 1987, **47**.

[15] B. Hess and A. Boiteux, *Ber. Bunsen Ges.* 84:346, 392 (1980);

[16] F. Hoppensteadt, *Mathematical Theories of Populations: Demographics*, 1975, Siam, Philadelphia.

[17] T. H. Johnson, S. R. Clark and D. Jaksch, *Phys. Rev. E*, 2010, **82**.

[18] W. Kermack and A. Mc Kendrick , A contribution to mathematical theory of epidemics, *Proc. Roy. Soc. Lond. A*, **115** (1927), pp. 700721.

[19] I. Z. Kiss and J. C. Miller and P. L. Simon, *Mathematics of Epidemics on Networks*, Springer-Verlag, Berlin.

[20] J. Kranz, *Epidemics of Plant disease*, 1990, Springer-Verlag, Berlin.

[21] A. Lančić, N. Antulov-Fantulin, M. Šikić and H. Štefančić, *Physica A Statistical Mechanics and its Applications*, 2011, **390**, pp 65-76.

[22] S. Lenhart and J. T. Workman, *Optimal control applied to biological models*, 2002, Chapman Hall, 6000 Broken Sound Parkway NW, Suite 300 Boca Raton.

[23] D. Li, P. Qin, H. Wang, C. Liu and Y. Jiang, *EPL (Europhysics Letters)*, 2014, **105**, 6.

[24] R. Marat and B.J. Manoel, *Computational and Applied Mathematics*, 2005, **24**, pp 65-81.

[25] M. Martcheva, *An Introduction to Mathematical Epidemiology*, 2010, Springer-Verlag, Berlin.

[26] F. Martinelli, S. Davino, S. Panno, G. Scuderi, P. Ruisi, P. Villa, D. Stroppiana, M. Boschetti, L.R. Goulart, C.E. Davis and A.M. Dandekar, *Agronomy for Sustainable Development*, 2015, **35**, 1, pp 1-25.

[27] J. L. Moore and , T. M. Rout and C. E. Hauser and D. Moro and M. Jones C. Wilcox and H. P. Possingham, *Biological Conservation*, 2010, **143**, pp 10681078.

[28] M.E.J. Newman, *SIAM Review* 45, 167 (2003)

[29] C. Nowzari, V. Preciado and G.J. Pappas, *IEEE CONTROL SYSTEMS MAGAZINE*, 2016, **12**, pp 2646.

[30] L. S. Pontryagin, V. G. Boltyanskii, R. V. Gamkrelidze, and E. F. Mishchenko, *The mathematical theory of optimal processes*, Wiley Interscience, New York, 1962.

[31] H. Santoso and B. Minasny, *Precision Agriculture*, 2011, **12**, pp 233248.

[32] S. P. Sethi and G. L. Thompson, *Optimal control theory: applications to management science and economics*, 2nd ed., Kluwer, Boston, 2006

[33] M. Shahul and H. R. Bivi and A. S. Paiko and A. Khairulmazmi and M. S. Akhtar , and A. S. Idris, *The Plant Pathology Journal*, 2016, **32**, pp 396-406.

[34] O. Sharomi and T. Malik, *Ann. Oper. Res.*, 2015

[35] K. Shea and the NCEAS Working Group on Population Management, *TREE*, 1998, **9**.

[36] C. J. Rhodes and R. M. Anderson, *Theoretical Population Biology*, 1997, **52**, pp 101-118.

[37] T. Tomé and R.M. Ziff, *PHYSICAL REVIEW E*, 2010, **82**.